Dynamically Heterogeneous Relaxation of Entangled Polymer Chains

Yuecheng Zhou[1] and Charles M. Schroeder[1,2,*]
[1]Department of Materials Science and Engineering, University of Illinois at Urbana-Champaign, Urbana, Illinois 61801, USA
[2]Department of Chemical and Biomolecular Engineering, University of Illinois at Urbana-Champaign, Urbana, Illinois 61801, USA

(Received 17 April 2018; published 26 June 2018)

Stress relaxation following deformation of an entangled polymeric liquid is thought to be affected by transient reforming of chain entanglements. In this work, we use single molecule techniques to study the relaxation of individual polymers in the transition regime from unentangled to entangled solutions. Our results reveal the emergence of dynamic heterogeneity underlying polymer relaxation behavior, including distinct molecular subpopulations described by a single-mode and a double-mode exponential relaxation process. The slower double-mode timescale $\tau_{d,2}$ is consistent with a characteristic reptation time, whereas the single-mode timescale τ_s and the fast double-mode timescale $\tau_{d,1}$ are attributed to local regions of transient disentanglement due to deformation.

DOI: 10.1103/PhysRevLett.120.267801

Entangled polymeric liquids are ubiquitous in materials processing and have garnered broad interest in condensed matter physics for many years [1]. Topological constraints in entangled polymer solutions and melts result in a dramatic slow down in chain dynamics, which is commonly modeled using the classic tube theory by de Gennes [1] and Doi and Edwards [2]. The tube model relies on a mean-field approximation by considering a single polymer chain moving or reptating through a confinement potential due to obstacles created by neighboring chains [3,4]. Recent work has considered topological entanglements in a self-consistent manner at the level of microscopic forces [5], which avoids the *ad hoc* assumptions of a confining tube while fundamentally deriving an effective confinement potential for entanglements.

A fundamental question underlying polymer solutions and melts focuses on how stress relaxes in topologically entangled systems. Following a large deformation, the original Doi-Edwards model (D-E) assumes that polymers undergo a fast chain retraction along the confining tube, followed by a slow stress relaxation via reptation to relax nonequilibrium orientations due to the deformation. Although the original D-E model was successful in capturing some aspects of the physics of entangled polymer solutions [6,7], experimentally determined longest relaxation times τ_d for melts exhibit a molecular weight M dependence of $\tau_d \sim M^{3.4}$ [8–10], whereas the D-E model predicts a molecular weight dependence of M^3. To reconcile this discrepancy, the original tube theory was extended to include constraint release [11,12] and contour length fluctuations [13,14]. For large nonlinear deformations, the D-E model was further extended to account for chain stretching [15], and convective constraint release to account for dynamic release of entanglements in flow. Accurate treatment of these phenomena resulted in an advanced microscopic theory (Graham-Likhtman-McLeish-Milner (GLAMM) model) that captures a wide range of dynamic properties of entangled polymers [16].

In addition to theoretical modeling, entangled polymer solutions have been extensively studied using bulk experimental methods such as light scattering and rheometry [10,17,18]. In recent work, Wang *et al.* [19] used small-angle neutron scattering (SANS) to infer molecular relaxation in entangled polymer solutions following a large deformation. Interestingly, these results showed that the fast initial chain retraction step predicted by the D-E model following a step strain was absent from experiments. These findings and recent theoretical advances [5,20,21] have brought into question some of the fundamental assumptions of the classic D-E theory and have highlighted the need for new molecular-level studies of entangled polymer solutions [22]. Despite their utility in probing polymer dynamics, bulk experimental methods tend to average over large ensembles of molecules, thereby obscuring the role of molecular subpopulations.

Single molecule techniques allow for the direct observation of polymer chains in flow [23], thereby revealing dynamic heterogeneity and molecular subpopulations under nonequilibrium conditions. Single molecule fluorescence microscopy (SMFM) has been used to directly observe tubelike or reptative motion in highly entangled DNA solutions [24] and to measure the tube confining potential in entangled DNA solutions [25]. Polymer relaxation in unentangled DNA solutions was recently studied using SMFM [26,27], and single DNA relaxation in highly entangled solutions following a step strain in shear flow was studied by Teixeira *et al.* [28]. Despite recent progress, however, polymer relaxation dynamics in entangled solutions is not fully understood at the molecular level.

In this Letter, we study the relaxation dynamics of single DNA polymers in the crossover regime between semidilute

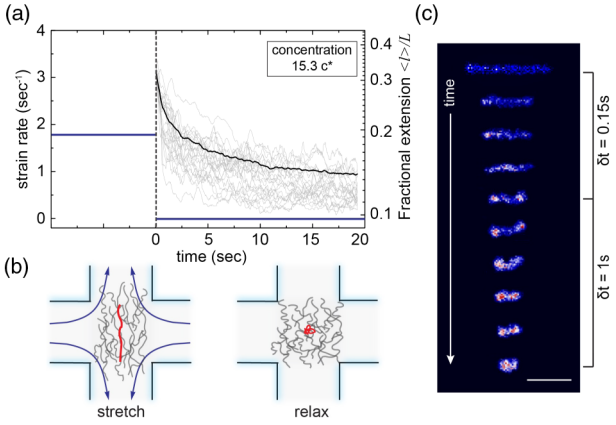

FIG. 1. Single molecule studies of polymer relaxation in entangled DNA solutions. (a) Flow deformation protocol and polymer relaxation process. At time $t = 0$, the flow is stopped and chains relax to equilibrium. Single molecule trajectories (gray) and ensemble averaged fractional extension (black) at $15.3\,c^*$. (b) Schematic of experiment showing a single fluorescently labeled tracer λ-DNA molecule (red) in a background of entangled DNA solution. (c) Snapshots of a single tracer DNA molecule relaxing in an entangled solution, showing double-mode relaxation behavior. Scale bar: 5 μm; δt is time between images.

unentangled and entangled solutions using SMFM (Fig. 1). Tracer bacteriophage λ-DNA molecules (48.5 kbp) are fluorescently labeled with a DNA intercalating dye (YOYO-1) and added to background solutions of unlabeled entangled λ-DNA (Supplemental Material [29]). In this way, we prepared a series of DNA solutions with polymer concentrations between $3.9\,c^*$ and $15.3\,c^*$ (Table S1 [29]), where $c^* = 50\ \mu g/\mathrm{mL}$ is the polymer overlap concentration for λ-DNA at 22.5 °C, which accounts for solvent quality and temperature [32]. Prior work has shown that λ-DNA transitions to entangled solution behavior around $c_e \approx 3c^*$ [32], where c_e is the critical entanglement concentration [33]. Solutions of λ-DNA between $3.9\,c^*$ and $15.3\,c^*$ correspond to approximately $n \approx 1$–12 entanglements per chain (Table S2 [29]).

A feedback-controlled microfluidic cross-slot device is used to generate a planar extensional flow (Fig. S1 [29]) [34,35]. Using this approach, single polymers are stretched to high degrees of extension ($l/L \approx 0.6$–0.7), where l is the end-to-end polymer extension and $L = 21\ \mu$m is the contour length of fluorescently labeled λ-DNA [Figs. 1(a) and 1(b)]. During the deformation step, polymers are exposed to at least $\epsilon = \dot{\epsilon}t = 10$ units of accumulated fluid strain in extensional flow, and deformation is performed at a dimensionless flow strength called the Weissenberg number $\mathrm{Wi} = \dot{\epsilon}\tau_d \gg 1$, where $\dot{\epsilon}$ is the strain rate and τ_d is the reptation time (discussed below). In this way, the flow induces a nonlinear deformation prior to relaxation. Following cessation of flow, the relaxation of a single tracer DNA molecule is observed as a function of time [Fig. 1(c)]. Flow field characterization including strain rate determination in entangled DNA solutions is performed via particle tracking velocimetry, with no elastic instabilities observed under these flow conditions (Fig. S3 [29]).

Polymer relaxation trajectories for the entire molecular ensemble are plotted for different solution concentrations in Fig. 2(a). Here, time is scaled by solvent viscosity η_0 to compare relaxation data between the low concentration $5.0\ c^*$ sample ($\eta_s = 18.1$ cP) and the remaining solution concentrations ($\eta_s = 0.95$ cP). Interestingly, for all polymer concentrations, we find that the ensemble-averaged relaxation trajectories cannot be fit by a single-mode exponential decay. Single exponential decay functions are commonly used to analyze polymer extension relaxation data in dilute polymer solutions ($c < c^*$) [23,36,37]

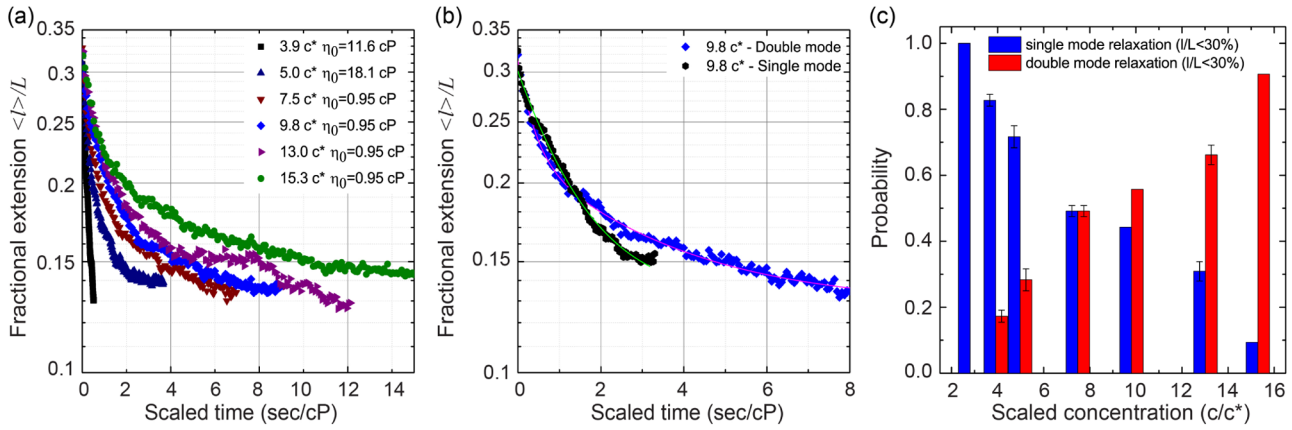

FIG. 2. Single molecule studies of polymer chain relaxation in entangled solutions reveal heterogeneous subpoplations. (a) Semilog plot of ensemble-averaged fractional extension $\langle l \rangle / L$ showing relaxation trajectories at five DNA concentrations ($5.0\,c^*$, $7.5\,c^*$, $9.8\,c^*$, $13.0\,c^*$, and $15.3\,c^*$; $N \geq 40$ molecules in each ensemble). (b) Molecular subpopulations corresponding to single-mode and double-mode relaxation trajectories for a representative solution concentration at $9.8\,c^*$. Ensemble averaged data for single- and double-mode trajectories are shown. (c) Probability distribution of single- and double-mode relaxation behavior at different polymer concentrations.

and semidilute unentangled solutions ($c^* < c < c_e$) [27]. On the other hand, our results show that the underlying molecular ensemble consists of two subpopulations, including polymers that exhibit either a single-mode or a double-mode exponential decay [Fig. 2(b) and Fig. S4 [29]]. To classify single polymers into these two different sets, each individual trajectory is fit to both functions, and the best fit is accepted with a suitable adjusted R-square value $\geq 90\%$ (Fig. S5 [29]). The single-mode relaxation time τ_s is determined by fitting the terminal 30% of the squared polymer extension $(l/L)^2$ to a single-mode exponential decay:

$$(l/L)^2 = A\exp(-t/\tau_s) + B \quad (1)$$

where A and B are numerical constants. The double-mode relaxation times $\tau_{d,1}$ and $\tau_{d,2}$ are obtained by fitting $(l/L)^2$ to a double-mode exponential decay:

$$(l/L)^2 = A_1\exp(-t/\tau_{d,1}) + A_2\exp(-t/\tau_{d,2}) + B \quad (2)$$

where A_1, A_2, and B are numerical constants.

Molecular ensembles corresponding to single-mode and double-mode relaxation behavior are shown in Fig. 2(b) and Fig. S4 [29]. Polymers exhibiting double-mode relaxation behavior exhibit an initially fast retraction with a characteristic timescale $\tau_{d,1}$, followed by slower relaxation with timescale $\tau_{d,2}$ before returning to an equilibrium coiled state. A histogram showing the probability of single-mode and double-mode relaxation behavior as a function of polymer concentration is shown in Fig. 2(c). Upon increasing polymer concentration from $2.8\,c^*$ to $15.3\,c^*$, the probability of single-mode relaxation behavior decreases, whereas the probability of double-mode behavior increases. The emergence of multiple molecular subpopulations is consistent with the gradual transition from the semidilute unentangled regime ($c < c_e$) to the semidilute entangled regime ($c > c_e$) at a critical entanglement concentration $c_e \approx 3c^*$. This value of c_e is consistent with prior work from bulk shear rheology of DNA [32] and single molecule measurements of polymer diffusion [38]. At relatively high polymer concentrations ($c = 15.3\ c^* \approx 5.1c_e$), nearly all relaxation trajectories exhibit double-mode relaxation behavior, which is consistent with prior observations on highly entangled λ-DNA solutions [28].

We quantitatively determined the single-mode relaxation times τ_s and double-mode relaxation times $\tau_{d,1}$ and $\tau_{d,2}$ from our experiments (Table S2 [29]). In this way, we observe clear power-law scaling behavior for the longest relaxation times as a function of scaled concentration c/c^* across a wide range of polymer concentrations, as shown in Fig. 3. Results from single molecule experiments are compared to longest relaxation times of entangled λ-DNA solutions measured from bulk shear rheology (based on a relaxation time λ from zero-shear viscosity η_0) [32], single molecule experiments following cessation of shear flow

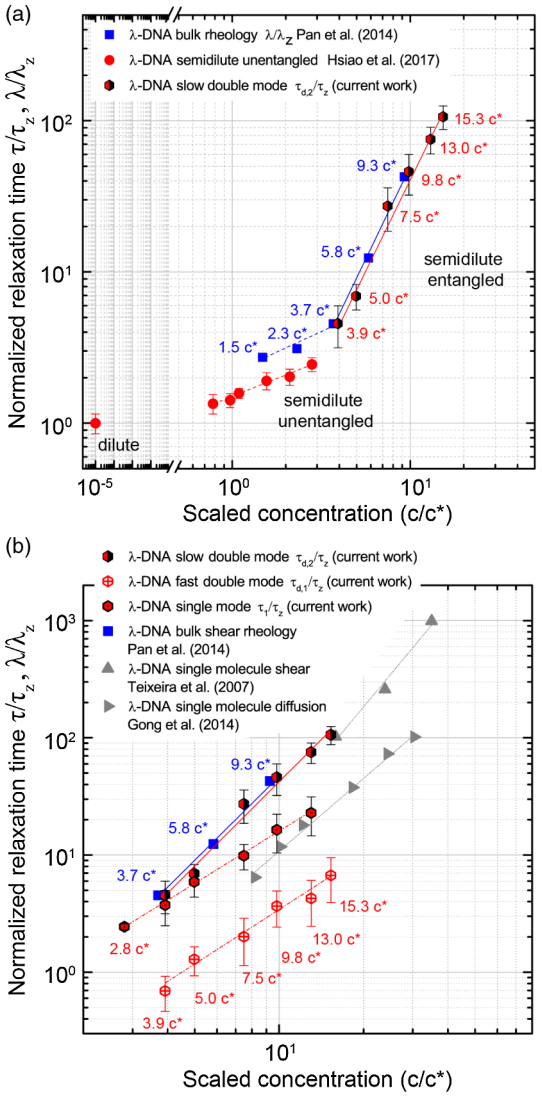

FIG. 3. Normalized longest relaxation times τ/τ_z and λ/λ_z as a function of scaled polymer concentration c/c^*. (a) Power-law relaxation time scaling behavior across the semidilute unentangled and entangled regimes. (b) Characteristic longest relaxation times in the entangled regime.

[28], and single polymer diffusion measurements [39]. For bulk experiments and single molecule measurements, the relaxation times λ and τ are normalized by the longest polymer relaxation time in the dilute limit λ_z and τ_z, respectively, and plotted as a function of scaled concentration c/c^* in Fig. 3.

Figure 3(a) shows the concentration-dependent power-law scalings of the longest relaxation times across the semidilute unentangled ($c^* < c < c_e$) and entangled regime ($c > c_e$). In the semidilute unentangled regime, the longest relaxation time scales with polymer concentration as $\tau/\tau_z \sim (c/c^*)^{0.48}$, as previously reported [27]. In the entangled regime, the relaxation behavior shows a dramatic slow down in dynamics. Here, the slower double-mode timescale $\tau_{d,2}$ exhibits a power-law scaling consistent

with the characteristic reptation time for semidilute entangled polymer solutions [3,4]. In particular, we find $\tau_{d,2}/\tau_z \sim (c/c^*)^{2.4}$ from single molecule experiments, which compares favorably with relaxation time scalings from bulk shear rheological experiments $\lambda/\lambda_z \sim (c/c^*)^{2.4}$ [32]. In entangled polymer melts, experiments [9] show that the reptation time τ_d exhibits a power-law scaling with polymer molecular weight M such that

$$\tau_d \sim M^{3.4}. \tag{3}$$

On the other hand, in entangled polymer solutions, polymer concentration and solvent quality both play a role on the reptation time τ_d. Scaling theory can be used to derive the concentration and solvent quality dependence of τ_d [4] (Supplemental Material [29]), such that

$$\tau_d = \frac{\tau_z}{(N_e(1))^{1.4}} \left(\frac{c}{c^*}\right)^{(3.4-3\nu)/(3\nu-1)} (zN^{-0.5})^{6\nu-5.8} (z^{1.4})^{2\nu+1} \tag{4}$$

where τ_z is the polymer relaxation time in the dilute limit, ν is the effective excluded volume coefficient, N is the number of statistical steps in the polymer (Kuhn segments), and $N_e(1)$ is the number of Kuhn steps in one entanglement strand in a melt. Moreover, z is the chain interaction parameter which is a measure of solvent quality (Supplemental Material [29]) [4]. Briefly, $z = k(1 - T_\theta/T)\sqrt{M}$, where M is polymer molecular weight and the constant k has been determined for DNA solutions using a combination of light scattering and brownian dynamics (BD) simulations [32], thereby enabling calculation of z for any M and T. For our experiments on λ-DNA conducted at $T = 22.5\,°\mathrm{C}$, we find $z \approx 0.71$, which corresponds to the lower limit of the good solvent regime [40].

Given that the reptation time τ_d scales with concentration as $\tau_d \sim (c/c^*)^{(3.4-3\nu)/(3\nu-1)}$ for entangled solutions and $\tau_{d,2} \sim (c/c^*)^{2.4}$ from our data, we determined an effective excluded volume exponent $\nu \approx 0.57$, which is consistent with good solvent conditions. Figure 3(b) also shows prior single molecule experimental data from Teixeira *et al.* [28], where double-mode relaxation behavior following shear flow deformation was observed at high DNA concentrations ($16\,c^*$–$35\,c^*$). Analysis of these prior data shows $\tau_{d,2} \sim (c/c^*)^{2.9}$, which is a steeper concentration dependence than the current work and corresponds to an effective excluded volume exponent of $\nu \approx 0.53$, which is closer to the expected scalings for Θ-solvent conditions [4,26]. Interestingly, the experiments of Teixeira *et al.* [28] were performed at $T = 18\,°\mathrm{C}$, such that the chain interaction parameter $z \approx 0.3$, suggesting near Θ-solvent conditions. Together, these data show the sensitivity of polymer relaxation behavior to experimental conditions for entangled polymer solutions.

The fast double-mode relaxation time $\tau_{d,1}$ exhibits a weaker power-law concentration dependence compared to the slow double-mode time $\tau_{d,2}$, such that $\tau_{d,1}/\tau_z \sim (c/c^*)^{1.5}$ [Fig. 3(b)]. Interestingly, the numerical values of $\tau_{d,1}$ are on the order of the Rouse time $\tau_R = 6R_G^2/3\pi^2 D_G^2$ [2] for λ-DNA (Table S2 [29]), where R_G is the radius of gyration determined from universal scaling relations for DNA [32] and D_G is the center-of-mass diffusion coefficient determined in prior single molecule experiments [41]. In this way, we determined a Rouse time $\tau_R = 0.3$ sec for λ-DNA at $T = 22.5\,°\mathrm{C}$ in a solvent viscosity $\eta_s = 1.0$ cP, which is consistent with prior estimates of τ_R [25]. Here, the Rouse time τ_R corresponds to the leading order time constant, but of course, higher order harmonics exist in a true Rouse spectrum. From this view, we hypothesize that $\tau_{d,1}$ corresponds to a timescale associated with a Rouse-like chain recovery or chain retraction following the nonlinear chain stretching step. A similar fast initial stress relaxation following a large uniaxial extensional deformation has also been observed in entangled polymer solutions [42,43] and melts [44] using bulk methods.

However, despite the apparent similarity to Rouse-like chain behavior, our data show that the fast double-mode relaxation time $\tau_{d,1}$ is concentration dependent, unlike a true Rouse-like response. These results suggest that the initial fast retraction step slows down as the local polymer concentration increases, which could occur due to increasing intermolecular friction due to nearby polymer chains. At longer times, entanglements reform in this molecular subpopulation, and the polymer chain transitions to a reptative relaxation process described by $\tau_{d,2}$.

Single molecule experiments further reveal an additional relaxation time τ_s, which emerges through a different molecular subpopulation in the ensemble. The single-mode relaxation time exhibits a power-law concentration scaling such that $\tau_s/\tau_z \sim (c/c^*)^{1.5}$. Although $\tau_{d,1}$ and τ_s show nearly the same power-law scaling with concentration, τ_s is approximately a factor of 5 larger than $\tau_{d,1}$ (Table S2 [29]), which suggests a different physical origin for τ_s compared to $\tau_{d,1}$. We conjecture that τ_s corresponds to the timescale of a polymer chain relaxation in a locally unentangled environment in the polymer solution. For this molecular subpopulation, polymer chains experience no chain-chain entanglements during the relaxation event, yet they may experience enhanced intermolecular interactions with an associated increase in chain friction during the relaxation process relative to semidilute unentangled solutions. Interestingly, locally unentangled behavior only exists in the transition regime from semidilute unentangled to semidilute entangled solutions [Fig. 2(c)]. At high polymer concentrations ($c \geq 16\,c^*$), the single-mode relaxation behavior is absent. These results are further supported by bulk shear rheology measurements on our entangled

DNA solutions, where an entanglement plateau emerges at 5.0 c^* and is clearly observed around 15 c^* (Fig. S6 [29]).

Our single molecule experiments reveal several intriguing features of polymer chain relaxation following a nonlinear deformation. In the lightly entangled regime, our results reveal two distinct molecular subpopulations exhibiting single-mode and double-mode exponential relaxation behavior. We conjecture that these two distinct behaviors correspond to different molecular relaxation pathways, such that the slow double-mode timescale $\tau_{d,2}$ is attributed to reptation, whereas the fast double-mode relaxation time $\tau_{d,1}$ is attributed to fast initial chain retraction step immediately following deformation. The original D-E theory postulates that a fast chain retraction step occurs immediately following deformation that serves to restore the initial primitive path length, with the net effect of a step deformation as orienting strands in a chain without stretching them. Our results are qualitatively consistent with a fast retraction step followed by a slow relaxation process, at least to the extent that the initial retraction step appears to significantly reduce polymer stretch. However, we find that the fast double-mode relaxation time $\tau_{d,1}$ is a function of concentration, which differs from a true Rouse-like response. On the other hand, we hypothesize that the single-mode time τ_s emerges from local regions of the polymer solution that have become transiently unentangled due to the strong deformation, and remain unentangled during the relaxation process. These results suggest that an apparently well-mixed polymer solution may be entangled at equilibrium and can become transiently disentangled upon exposure to strong deformation. As polymer concentration is increased ($c \gg c^*$), the propensity for transient disentanglements to occur within the solution decreases.

An intriguing question is how our results can be compared to recent SANS experiments on entangled polymer relaxation [19]. The results of Wang *et al.* showed no evidence of chain retraction by analyzing the anisotropic components of a structure factor, which is bulk quantity averaged over a large ensemble. In our experiments, we directly measure transient chain stretch during relaxation, which could be interpreted as a measure of chain anisotropy, but polymer stretch is clearly different from a wave vector-dependent structure factor. Future work may enable more direct comparisons between molecular-level and bulk measurements of entangled polymers.

We thank Kenneth Schweizer for helpful discussions and Simon Rogers and Johnny Lee for rheometeric measurements. This work was supported by NSF CBET 1604038 for C. M. S. and a PPG-MRL graduate research assistantship award for Y. Z.

*cms@illinois.edu

[1] P. G. de Gennes, Macromolecules **9**, 587 (1976).
[2] M. Doi and S. F. Edwards, *The Theory of Polymer Dynamics* (Oxford University Press, Oxford, UK, 1986), p. 391.
[3] P. G. de Gennes, Macomolecules **9**, 594 (1976).
[4] M. Rubinstein and R. H. Colby, *Polymer Physics* (Oxford University Press, Oxford, UK, 2003) p. 440.
[5] K. S. Schweizer and D. M. Sussman, J. Chem. Phys. **145**, 214903 (2016).
[6] T. P. Lodge, N. A. Rotstein, and S. Prager, in *Advances in Chemical Physics*, edited by I. Prigogine and S. A. Rice (John Wiley & Sons, New York, 1990), Vol. 79, pp. 1–132.
[7] T. C. B. McLeish, Adv. Phys. **51**, 1379 (2002).
[8] J. D. Ferry, *Viscoelastic Properties of Polymers*, 3rd ed. (John Wiley & Sons, New York, 1980).
[9] T. P. Lodge, Phys. Rev. Lett. **83**, 3218 (1999).
[10] R. G. Larson, *The Structure and Rheology of Complex Fluids* (Oxford University Press, New York, 1999).
[11] W. Graessley, in *Synthesis and Degradation Rheology and Extrusion*, Advances in Polymer Science (Springer, Berlin, Heidelberg, 1982), Vol. 47, pp. 67–117.
[12] J. L. Viovy, M. Rubinstein, and R. H. Colby, Macromolecules **24**, 3587 (1991).
[13] M. Doi, J. Polymer Sci. **21**, 667 (1983).
[14] S. T. Milner and T. C. B. McLeish, Phys. Rev. Lett. **81**, 725 (1998).
[15] G. Marrucci and N. Grizzuti, Gazz. Chim. Ital. **118**, 179 (1988).
[16] R. S. Graham, A. E. Likhtman, T. C. B. McLeish, and S. T. Milner, J. Rheol. **47**, 1171 (2003).
[17] H. Watanabe, Prog. Polym. Sci. **24**, 1253 (1999).
[18] M. Adam and M. Delsanti, J. Phys. **44**, 1185 (1983).
[19] Z. Wang, C. N. Lam, W.-R. Chen, W. Wang, J. Liu, Y. Liu, L. Porcar, C. B. Stanley, Z. Zhao, K. Hong, and Y. Wang, Phys. Rev. X **7**, 031003 (2017).
[20] D. M. Sussman and K. S. Schweizer, Phys. Rev. Lett. **109**, 168306 (2012).
[21] D. M. Sussman and K. S. Schweizer, Macromolecules **45**, 3270 (2012).
[22] T. T. Falzone and R. M. Robertson-Anderson, ACS Macro Lett. **4**, 1194 (2015).
[23] C. M. Schroeder, J. Rheol. **62**, 371 (2018).
[24] T. T. Perkins, D. E. Smith, and S. Chu, Science **264**, 819 (1994).
[25] R. M. Robertson and D. E. Smith, Phys. Rev. Lett. **99**, 126001 (2007).
[26] Y. Liu, Y. Jun, and V. Steinberg, J. Rheol. **53**, 1069 (2009).
[27] K.-W. Hsiao, C. Samsal, J. R. Prakash, and C. M. Schroeder, J. Rheol. **61**, 151 (2017).
[28] R. E. Teixeira, A. K. Dambal, D. H. Richter, E. S. G. Shaqfeh, and S. Chu, Macromolecules **40**, 2461 (2007).
[29] See Supplemental Material at http://link.aps.org/supplemental/10.1103/PhysRevLett.120.267801, which includes [30,31], for studies of contour length for λ-DNA after labeling and relaxation times given by the Zimm model.
[30] B. Kundukad, J. Yan, and P. S. Doyle, Soft Matter **10**, 9721 (2014).
[31] B. H. Zimm, J. Chem. Phys. **24**, 269 (1956).
[32] S. Pan, D. A. Nguyen, T. Sridhar, P. Sunthar, and J. R. Prakash, J. Rheol. **58**, 339 (2014).
[33] W. W. Graessley, Polymer **21**, 258 (1980).
[34] M. Tanyeri and C. M. Schroeder, Nano Lett. **13**, 2357 (2013).

[35] A. Shenoy, C. V. Rao, and C. M. Schroeder, Proc. Natl. Acad. Sci. U.S.A. **113**, 3976 (2016).
[36] Y. Zhou and C. M. Schroeder, Phys. Rev. Fluids **1**, 053301 (2016).
[37] T. T. Perkins, D. E. Smith, and S. Chu, Science **276**, 2016 (1997).
[38] R. M. Robertson and D. E. Smith, Macromolecules **40**, 3373 (2007).
[39] Z. Gong and J. R. C. Van Der Maarel, Macromolecules **47**, 7230 (2014).
[40] C. Samsal, K.-W. Hsiao, C. M. Schroeder, and J. R. Prakash, J. Rheol. **61**, 169 (2017).
[41] R. M. Robertson, S. Laib, and D. E. Smith, Proc. Natl. Acad. Sci. U.S.A. **103**, 7310 (2006).
[42] P. K. Bhattacharjee, D. A. Nguyen, G. H. McKinley, and T. Sridhar, J. Rheol. **47**, 269 (2003).
[43] Q. Huang and H. K. Rasmussen, J. Rheol. **60**, 465 (2016).
[44] J. K. Nielsen, H. K. Rasmussen, and O. Hassager, J. Rheol. **52**, 885 (2008).